JOURNAL OF SOLID STATE CHEMISTRY 112, 387–391 (1994)

Nonisothermal Site Saturation during Transformations of Zn_2SiO_4

Chung-Cherng Lin and Pouyan Shen[1]

Institute of Materials Science and Engineering, National Sun Yat-Sen University, Kaohsiung, Taiwan 804, Republic of China

Received June 30, 1993; in revised form November 29, 1993; accepted December 2, 1993

Determination of site saturation for transformations in an amorphous or crystalline matrix of nanometer size can be accomplished quantitatively using nonisothermal thermal analysis at various heating rates. This is demonstrated by the transformations kinetics of gel-produced Zn_2SiO_4 fitted to the equation of Matusita *et al.* Regardless of the heating rates adopted, both the crystallization and the subsequent $\beta \rightarrow \alpha$ transformation involve mainly bulk nucleation (with corresponding site saturation at volume fractions (x) $\approx$ 63 and 30%, respectively) followed predominantly by one-dimensional growth. The difference in the extent of site saturation in the two transformations is attributed mainly to the numbers of available sites in the corresponding matrix, most likely SiO_4 and lattice imperfections for the amorphous gel and the crystalline β phase, respectively. © 1994 Academic Press, Inc.

1. INTRODUCTION

Transformation kinetics during continuous cooling can be approached from isothermal transformation data when nucleation occurs early in the reaction, i.e., site saturation due to a limited number of sites for nucleation (1). The application equation for a nonisothermal transformation was first suggested by Kissinger (2). Since that time, nonisothermal thermal analysis has become a popular and convenient means for the kinetic studies on the chemical reactions and crystallization of glasses.

A number of works have been contributed to improving nonisothermal differential thermal analysis (DTA) and differential scanning calorimetry (DSC) (3–8) or nonisothermal thermogravimetric analysis (TGA) (9–12) methods of calculating the activation energy for chemical reaction or crystal growth. Besides the method suggested by Sichen and Seetharaman (12), who studied the solid–gas interfacial reaction and diffusion, all of these methods are based on the Avrami treatment (or the Johnson–Mehl–Avrami equation) of transformation kinetics or on the assumption of the first-order reaction. A critical review discussing the applications and limitations of the methods has been given by Yinnon and Uhlmann (13). As a matter of fact, these methods cannot be directly applied to the crystallization of amorphous materials and the physical meaning of the activation energies thus obtained is not clear because crystallization involves a nucleation and growth process rather than the nth-order reaction. Furthermore the original JMA equation was derived for isothermal transformation, not for the nonisothermal case.

A method of analyzing the nonisothermal crystallization kinetics on the basis of the nucleation and growth process with emphasis on the crystallization mechanism has been developed by Matusita and Sakka (14–16) and Matusita *et al.* (17). According to Matusita *et al.* (17), the activation energy and the appropriate nucleation-growth mechanism were estimated by the equation

$$\ln[-\ln(1-x)] = -n \ln \phi - 1.052mE_c/RT + \text{const}, \quad [1]$$

where E_c is the apparent activation energy for crystal growth, n and m are the numerical factors depending on the nucleation process and growth mechanism, x is the volume (or mole) fraction of the new phase, ϕ is the heating rate of DTA or DSC runs, and R and T are the gas constant and absolute temperature, respectively. In the derivation of this equation, no restriction on the form of sample was given (14) although bulk melt was easier for microstructural confirmation and surface nucleation may become important for powdery samples. It has been pointed out by morphology observations that $n = m + 1$ when the nuclei formed during the heating at the constant rate are dominant, but $n = m$ if the nuclei formed in the previous heat treatment before thermal analysis run are dominant (14). The correlation between crystallization mechanism and values of n and m is shown in Table 1 for the case of $n = m + 1$. It is clear from this table that $m = 1$ is valid for both bulk nucleation ($n = 2$) and surface nucleation ($n = 1$) processes. Ambiguities of this criterion may arise if site saturation occurs above a critical temperature during heating. In such as case, bulk-site saturation followed by one-dimensional growth (i.e., $n = 2$ before site saturation but appeared to be 1 after site saturation above the critical temperature) can possibly be mistaken from the case of surface nucleation process ($n = m =$

[1] To whom correspondence should be addressed.

0022-4596/94 $6.00

1). Differentiation of nucleation from growth for a thermale vent is therefore crucial for a better understanding of nonisothermal transformation kinetics. The nucleation kinetics were commonly inferred from the overall transformation kinetics when the growth front can be readily monitored. Unfortunately this approach is not practical for nonisothermal transformation of powdery samples; therefore determination of site saturation appeared to be the alternative, if not the only, choice for such a differentiation.

In this work, nonisothermal thermal analysis of nanometric Zn_2SiO_4 powders was employed to show that site saturation, which corresponds to a fixed fraction of transformation under the condition of instantaneous nucleation, indeed occurs for both crystallization and $\beta \rightarrow \alpha$ transformation at various heating rates and to demonstrate that the kinetics data can then be used to decipher the mechanism of nucleation and growth using Eq. [1]. The mechanism and apparent activation energy of the two transformations upon heating are also of engineering and fundamental interests to the phosphor applications of Zn_2SiO_4.

2. EXPERIMENTAL

The starting sample ZS_1 is amorphous Zn_2SiO_4 consisting of powders ca. 10 ~ 20 nm in size as revealed by vibrational spectroscopy and transmission electron microscope (18). This material was prepared by a sol–gel route from TEOS and diethylzinc using a two-stage hydrolysis–condensation process (catalyzed by 3 N HNO_3 and then 0.1 M NH_4OH; refer to Lin and Shen (18) for further details). Simultaneously and in static air, both DTA and TGA (Netzsch STA409) were brought up to 1000°C against the reference (α-Al_2O_3) and at heating rates of 2.5, 5, 7.5, and 10°C/min. (The DTA peaks of $\beta \rightarrow \alpha$ transition were not recognized when the heating rate was much lower, e.g., 1°C/min, or higher, e.g., 20°C/min.) The same amount (50 mg) of sample and reference material were put separately in alumina crucibles (5 and 7 mm in inner and outer diameter, respectively) for each run. The thermal events of transformations were recorded using an S-type (Pt10%Rh) thermocouple.

The integrated area of DTA peaks and the shift of peak temperatures due to the changes in heating rates were used to infer the kinetics of transformation. Each DTA datum was based on the average of three independent runs. The hypothesis that site saturation corresponds to a fixed fraction of transformation was examined on the possible slope break of the plot of $\ln[-\ln(1 - x)]$ vs $1/T$ using Eq. [1] and at various heating rates. The activation energy was estimated from the same plot at a specific heating rate, while the n value was obtained from the plot of $\ln[-\ln(1 - x)]$ against $\ln \phi$ at a specific temperature. On the basis of these plots, the appropriate nucleation and growth mechanisms can then be inferred.

3. RESULTS AND DISCUSSION

3.1. Thermal Events

The DTA and TGA traces for a heating rate of 10°C/min are shown representatively in Fig. 1. Crystallization into β phase at about 722°C and then transformation into α phase at 919°C are manifested by the sharp exothermic peaks on the DTA trace and the accompanying weight loss on the TGA trace (18). It is noteworthy that the specific surface areas measured after holding for 15 min at 600 and 800°C are 51.6 and 9.5 m^2/g, respectively (18). The weight loss and surface area change might have contributed slightly to heat release; however, they should not disturb the kinetics data for the two transformations as discussed below.

The weight loss in TGA during transition has been attributed to the dehydration of sample (18). It is possible that the formation of H_2O can slightly enlarge the DTA peak area. Nevertheless this factor can be excluded as a disturbance to the experimental data because other Zn_2SiO_4 gels, which were more condensed under a higher NH_4OH, showed similar transformation kinetics but with much less weight loss (19).

As indicated by the slope of the DTA curve (Fig. 1) the reduction of specific surface area (i.e., agglomeration of the powders and hence the release of excess surface energy) should shift the DTA baseline toward the exothermic side in a temperature range rather than at a specific temperature. Besides, the change of the specific surface area during a DTA run at 10°C/min should be much less than that measured after isothermal holding for a considerable time period (18). Thus the estimation of the percent-

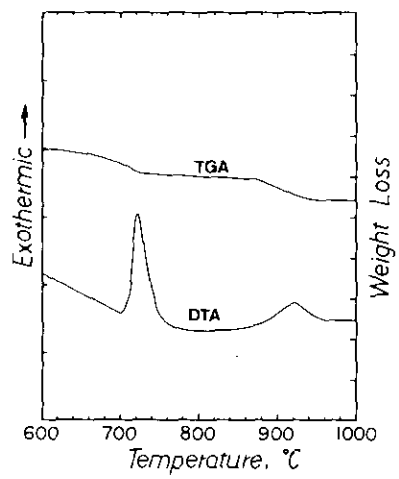

FIG. 1. DTA and TGA curves of sample ZS_1 in static air (heating rate = 10°C/min). Full scale is 10 mg for TGA and 30 μV for DTA.

age of transformations from the areas of the DTA peaks should not be interfered by the surface area change.

3.2. Crystallization of β Phase

A plot of $\ln[-\ln(1-x)]$ vs $\ln\phi$ for the as-formed sample ZS_1 at several temperatures is shown in Fig. 2. It is found that the negative slope (i.e., n) decreases with increasing temperature, in contrast to a constant value reported for other glass systems, e.g., As–Sb–Se (20), Se–Te (21), and Se–Ge–Sb, (22). Since the n value is larger than 1 except above 730°C, bulk nucleation should be dominant following the arguments of Refs. (15, 17) (refer also to Table I) but nucleation at the particle surface cannot be excluded. An n value near 1.0 above 730°C should not be regarded as due to a surface nucleation process. This is due to the fact that surface has a higher energy than the interior of a particle and the saturation of a type of site; e.g., bulk site limits all further nucleation at sites of lower dimensionality, e.g., grain boundary site (23). The latter criterion holds also for nonisothermal transformation when the temperature range of the DTA peak is narrow as in the present case. We suggest that site saturation above a critical temperature which is in accordance with the slope breaks on the $\ln[-\ln(1-x)]$ vs $1/T$ plot (see below) accounts for the temperature dependence of n values.

Figure 3 is a plot of $\ln[-\ln(1-x)]$ against the reciprocal temperature for several heating rates. A break in the slope ($-1.052\,mE_c/R$), i.e., a smaller mE_c value above a critical temperature, occurs for each heating rate. It is noted in the present plot that the slope breaks at nearly the same volume fraction ($x \approx 0.63$) for varied heating rates (Fig. 2). A constant x value is in accordance with the saturation of nucleation sites if growth is limited before site saturation, which is valid for a high heating rate and a small

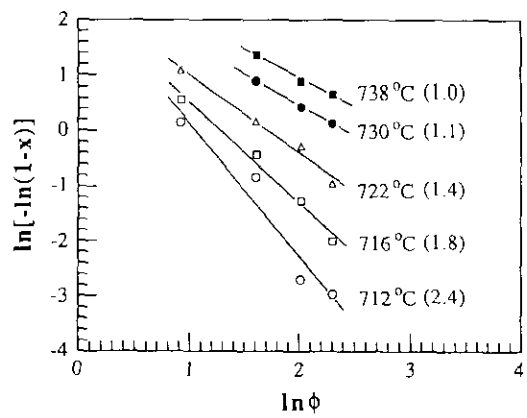

FIG. 2. $\ln[-\ln(1-x)]$ vs $\ln\phi$ plot for crystallization of sample ZS_1 at five temperatures, where ϕ is the heating rate, x is the fraction of crystallization at the temperature of interest, and the negative slope of the plot is the n value (given in parentheses) which is related to the transformation mechanism (refer to Table 1).

TABLE 1
Correlation between Crystallization Mechanism and Values of n and m

Crystallization mechanism	n	m
Bulk nucleation		
Three-dimensional growth	4	3
Two-dimensional growth	3	2
One-dimensional growth	2	1
Surface nucleation	1	1

Note. Taken from Matusita and Sakka (15, 17). $n = m$ is also valid for the case of site saturation (refer to text).

particle size as in the present case. A large volume fraction ($x \approx 0.63$) for site saturation suggests that surface nucleation was overwhelmed by bulk nucleation. This interpretation is also consistent with the argument of n value. Other factors of slope break can be excluded as discussed in Section 3.4.

The bulk nucleation sites in gel may be the structural units SiO_4 or the SiO_4–ZnO_4 clusters which also exist in the β phase. During heat treatment, structural units such as Si_2O_7 and Si_2O_5 which resulted from polycondensation of SiO_4 during the preparation of sample should decompose into SiO_4. Decomposition of polymerized silicate units into isolated SiO_4 tetrahedra has also been observed during preparation of the lead orthosilicate glass from melt and has been attributed to a disproportionation reaction (24). The formation of SiO_4 has also been suggested as the atomic-scale initiation of phase separation before crystallization (25). It follows that the bulk nucleation sites in the present gel are most likely the SiO_4. Since the n values are proximate to 1 above the temperature of site saturation, the nonisothermal growth of β phase is

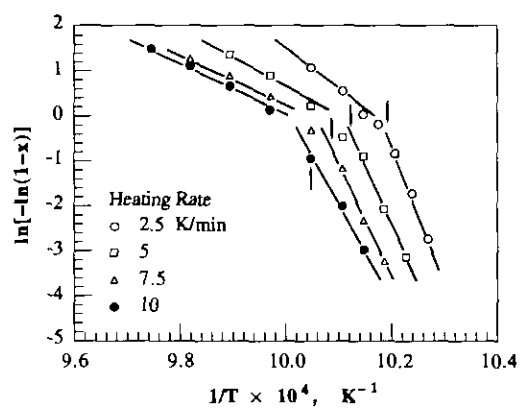

FIG. 3. Variation of $\ln[-\ln(1-x)]$ with reciprocal temperature during crystallization of sample ZS_1 for four heating rates, the arrows indicate the DTA peak temperatures.

predominantly one-dimensional under this condition (i.e., $n = m = 1$).

3.3. $\beta \rightarrow \alpha$ Transformation

Similar to the crystallization of β phase, the n values of the $\ln[-\ln(1-x)]$ vs $\ln \phi$ plot decrease with increasing temperature (Fig. 4). The $\ln[-\ln(1-x)]$ vs $1/T$ plots at specified heating rates show slope break (i.e., site saturation) at about $x = 0.30$ for $\beta \rightarrow \alpha$ transformation (Fig. 5). A easy site saturation for $\beta \rightarrow \alpha$ transformation compared with crystallization can be attributed to a smaller number of bulk nucleation sites for the former. The most likely nucleation sites in β phase are lattice imperfections, which commonly serve as heterogeneous nucleation sites for both reconstructive and topotactic change in a crystalline matrix. Attempts have been made to study the defects of β phase by transmission electron microscopy; however, irradiation damage interferes with detailed characterization. For the same reasons as those suggested in a previous section for crystallization, the dominant transformation mechanism for $\beta \rightarrow \alpha$ is bulk nucleation followed by one-dimensional growth.

It has indeed been observed that willemite (i.e., α-Zn_2SiO_4) single crystal preferentially grows along its c-axis (26–28) and forms spherulite in glass matrix (29), i.e., one-dimensional growth. However, the growth of β phase from amorphous particle and α phase from β-phase particle may not always be one-dimensional. Complexity may arise from the polytypism and twinning which take place during the formation of β phase (30, 31). In addition, a habit plane, such as (1120) of willemite and (001) of β phase (30), may modify the growth behavior. Both the β and α particles have a faceted surface (32) although they commonly appeared to be more or less spherical. It is not clear if such a surface facet facilitates growth during transformations.

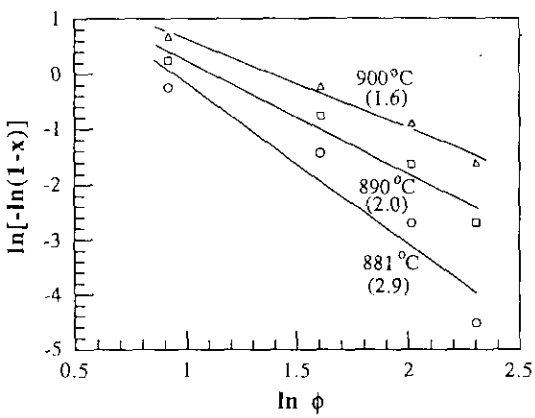

FIG. 4. $\ln[-\ln(1-x)]$ vs $\ln \phi$ plot for $\beta \rightarrow \alpha$ transition of sample ZS_1 at three temperatures; the numerical values in parentheses are the negative slopes, i.e., the n values.

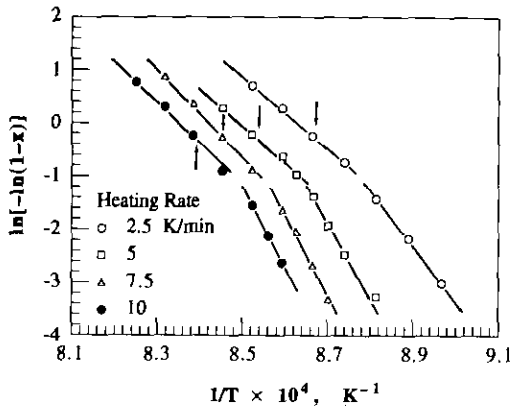

FIG. 5. Variation of $\ln[-\ln(1-x)]$ with reciprocal temperature during $\beta \rightarrow \alpha$ transition for four heating rates; the arrows indicate the DTA peak temperatures.

It has been suggested that the $\beta \rightarrow \alpha$ transformation of zinc orthosilicate can proceed either by a reconstructive transformation involving total disruption and reconstitution of the structure or by a mechanism involving only relatively minor changes analogous to topotactic changes (30, 31). In spite of a large number of nucleation sites in β phase, its transformation product, α-phase, remained nearly the same size (18). This is in favor of a topotactic change, although the considerable heat of reaction accompanying $\beta \rightarrow \alpha$ transition as indicated by the DTA trace (Fig. 2) suggested that bond reorganization was involved.

Regardless of the n and m values and the heating rates, the apparent activation energy estimated from the $\ln[-\ln(1-x)]$ vs $1/T$ plot is lower for crystallization than $\beta \rightarrow \alpha$ transformation. It should be noted that regardless of heating rate, the DTA peak temperatures (T_p) appeared before the slope break for crystallization (Fig. 3) but after the slope break for $\beta \rightarrow \alpha$ transformation (Fig. 5). Therefore the apparent activation energy obtained from the shift of T_p cannot be simply attributed to a growth process (i.e., site saturation was not always reached at peak temperature). Misinterpretation of activation energy for crystallization may also arise if the glass transition is shielded by a crystallization peak (33) or water in the sol–gel-derived sample lowers the kinetics barrier for crystallization as reported in other systems (34, 35).

3.4. Factors of a Slope Break for the $ln[-ln(1-x)]$ vs $1/T$ Plot

Slope break has been reported in this plot (19, 21, 36) or the isothermal Avrami plot (33, 37–39) for various glass compositions and crystals. This has been attributed to: (1) the hypothetical saturation of volume nucleation sites in the final stage of crystallization (33, 37), (2) the restriction of crystal growth by the small size of the particles (38), or (3) the surfacial nucleation prevailing over internal nucleation or other heterogeneities (39). The second fac-

tor can be excluded because both amorphous and β-Zn_2SiO_4 have nearly the same size (18), which should give one instead of two volume fractions x at two slope breaks. The third argument also has problems because the predominant mechanism for the present transformations is bulk nucleation followed by one-dimensional growth, rather than surface nucleation. Another factor of slope break, the change in growth dimensionality, is considered unlikely for small particle size. In any case, the main concern is the specified volume fractions x at slope breaks which favor the argument of site saturation in the present study.

4. CONCLUSIONS

Nucleation can be differentiated quantitatively from growth for transformations in an amorphous or crystalline matrix using nonisothermal thermal analysis of powdery samples at various heating rates. For example, nonisothermal studies of the crystallization and the subsequent $\beta \rightarrow \alpha$ transformation of gel-produced Zn_2SiO_4 powders lead to the following conclusions.

1. Site saturation for both transformations is supported by the fact that the slope (i.e., negative n value) of the plot of $\ln[-\ln(1 - x)]$ vs reciprocal temperature breaks at a specified volume fraction ($x \approx 63$ and 30% for crystallization and the subsequent $\beta \rightarrow \alpha$ transformation, respectively) regardless of heating rates.

2. An easier site saturation for $\beta \rightarrow \alpha$ transformation than crystallization is attributed mainly to the numbers of available sites in the corresponding matrix, most likely lattice imperfections and SiO_4 for the crystalline β phase and amorphous gel, respectively.

3. Both transformations involve predominantly one-dimensional growth.

ACKNOWLEDGMENTS

We thank Drs. A. C. Su and P. W. Kao for helpful discussions and a referee for comments.

REFERENCES

1. J. W. Cahn, *Acta Metall.* **4,** 572 (1956).
2. H. E. Kissinger, *J. Res. Natl. Bur. Stand.* **57,** 217 (1956).
3. H. E. Kissinger, *Anal. Chem.* **29,** 1702 (1957).
4. G. O. Piloyan, I. D. Ryabchikov, and O. S. Novikova, *Nature* **212,** 1229 (1966).
5. T. Ozawa, *Polymer* **12,** 150 (1971).
6. J. A. Augis and J. E. Bennett, *J. Thermal Anal.* **13,** 283 (1978).
7. A. Marotta, A. Buri, and G. L. Valenti, *J. Mater. Sci.* **13,** 2483 (1978).
8. A. Marotta, S. Saiello, F. Branda, and A. Buri, *J. Mater. Sci.* **17,** 105 (1982).
9. H. H. Horowitz and G. Metzger, *Anal. Chem.* **35,** 1464 (1963).
10. A. W. Coats and J. P. Redfern, *Nature* **201,** 68 (1964).
11. T. Ozawa, *Bull. Chem. Soc. Jpn.* **38,** 1881 (1965).
12. D. Sichen and S. Seetharaman, *Metall. Trans. B* **23,** 317 (1992).
13. H. Yinnon and D. R. Uhlmann, *J. Non-Cryst. Solids* **54,** 253 (1983).
14. K. Matusita and S. Sakka, *Phys. Chem. Glasses* **20,** 81 (1979).
15. K. Matusita and S. Sakka, *Thermochim. Acta* **33,** 351 (1979).
16. K. Matusita and S. Sakka, *J. Non-Cryst. Solids* **38/39,** 741 (1980).
17. K. Matusita, T. Komatsu, and R. Yokota, *J. Mater. Sci.* **19,** 291 (1984).
18. C. C. Lin and P. Shen, *J. Non-Cryst. Solids*, in press (1994).
19. C. C. Lin, "Synthesis, Phase Transformations, and Dissolution Behavior of Zinc Orthosilicate." Ph. D. thesis, Univ. Sun Yat-Sen, Taiwan, R.O.C., 1992.
20. S. Mahadevan, A. Giridhar, and A. K. Singh, *J. Non-Cryst. Solids* **88,** 11 (1986).
21. N. Afify, *J. Non-Cryst. Solids* **136,** 67 (1991).
22. N. Afify, M. A. Abdel-Rahim, A. S. A. El-Halim, and M. M. Hafiz, *J. Non-Cryst. Solids* **128,** 269 (1991).
23. J. W. Cahn, *Acta. Metall.* **4,** 449 (1956).
24. T. Furukawa, S. A. Brawer, and W. B. White, *J. Mater. Sci.* **13,** 268 (1978).
25. J. F. Stebbins, *J. Non-Cryst. Solids* **106,** 359 (1988).
26. M. Setoguchi and C. Sakamoto, *Yogyo Kyo Kai Shi* **83,** 428 (1975).
27. K. Kodaira, S. Ito and T. Matsushita, *J. Cryst. Growth* **29,** 123 (1975).
28. K. H. Klaska, J. C. Eck, and D. Pohl, *Acta Cryst. Sect. B* **34,** 3324 (1978).
29. F. H. Norton, *J. Am. Ceram. Soc.* **20,** 217 (1937).
30. H. F. W. Taylor, *Am. Mineral.* **47,** 932 (1962).
31. J. Williamson and F. P. Glasser, *Phys. Chem. Glasses* **5,** 52 (1964).
32. C. C. Lin and P. Shen, *Geochim. Cosmochim. Acta*, in press (1994).
33. P. Duhaj, D. Barancok, and A. Ondrejka, *J. Non-Cryst. Solids* **21,** 411 (1976).
34. C. J. R. Gonzalez-Oliver, P. S. Johnson and P. F. James, *J. Mater. Sci.* **14,** 1159 (1979).
35. J. Zarzycki, *in* "Nucleation and Crystallization in Glass," (J. H. Simmons, D. R. Uhlmann and C. H. Beall, Eds.), Advances in Ceramics, Vol. 4, pp. 204–217. Am. Ceram. Soc., Columbus, 1981.
36. L. J. Shelestak, R. A. Chavez, and J. D. Mackenzie, *J. Non-Cryst. Solids* **27,** 83 (1978).
37. J. Colmenero and J. M. Barandiarán, *J. Non-Cryst. Solids* **30,** 263 (1979).
38. R. F. Speyer and S. H. Risbud, *Phys. Chem. Glasses* **24,** 26 (1983).
39. W. D. Carlson, *J. Geol.* **91,** 57 (1983).